Pairing phase transitions in nuclear wave functions

Mihai Horoi[1] and Vladimir Zelevinsky[2]
[1]*Department of Physics, Central Michigan University, Mount Pleasant, Michigan 48859, USA*
[2]*Department of Physics and Astronomy and National Superconducting Cyclotron Laboratory, Michigan State University, East Lansing, Michigan 48824-1321, USA*
(Received 5 February 2007; published 3 May 2007)

The exact solution of the nuclear shell model is used for studying the phase transition from superfluid to normal Fermi-liquid as a function of the pairing strength, excitation energy (or temperature), nuclear spin and the presence of other types of residual interactions. The phase transition in a finite system is seen through the change of properties of individual wave functions.

DOI: 10.1103/PhysRevC.75.054303 PACS number(s): 21.60.Cs, 21.30.Fe

I. INTRODUCTION

Significant effects of nuclear pairing correlations are observed throughout the periodic table [1]. From the time of seminal papers by Bohr, Mottelson, and Pines [2] and Belyaev [3] it is well known that these correlations influence considerably all nuclear properties. The current progress in physics of nuclei far from stability requires better understanding of nuclear pairing as one of essential factors defining the limits of nuclear existence. This is also an important ingredient in physics of many other mesoscopic systems and astrophysics of neutron stars [4].

Approximations borrowed from macroscopic theory of superconductivity are routinely used to treat the pairing correlations in heavy nuclei. As a rule, the dynamics of fermion pairs are substituted by the average pairing condensate field Δ [standard Bardeen-Cooper-Schrieffer (BCS) theory or more elaborate Hartree-Fock-Bogoliubov (HFB) approach, where the pairing field is self-consistently created by a specific part of the particle interaction that corresponds to the maximum attraction, "pairing interaction"]. The bulk phase transition destroying superconductivity can be recognized by the disappearance of Δ. The condensate approximation violates particle number conservation and can be insufficient, especially in small systems, such as nuclei or metallic clusters. The fluctuations of the mean field become crucial in the region of the phase transition smeared by the small size effects [5–7]. Special methods to improve the mean field approach by restoring conservation laws and including pairing fluctuations were developed, see for example [8,9], and references therein.

With the monopole pairing interaction, the BCS solution is asymptotically exact in the thermodynamic limit of macroscopic systems. However the realistic interaction is much more diverse than simple pairing. Pairs can be formed in different quantum states, and the competition between different couplings may lead to their complicated interplay. The interaction contains other coherent components responsible for collective excitations (in nuclei—shape vibrations and deformation of the mean field). Incoherent parts of the interaction induce the stochastization of dynamics. As excitation energy and level density increase, the processes of collision-like mixing convert many-body stationary states into complicated superpositions of a very large number of simple configurations. In the BCS or HFB approaches, the incoherent interactions are neglected to the extent that they do not contribute to the mean field. In macroscopic systems these effects are presumably included in the Fermi-liquid renormalization of the quasiparticles. In the nuclear shell model, the additional interactions appear explicitly being responsible for the rapid growth of complexity of the eigenstates [10,11].

The models using the schematic pairing-type interactions [12] exhibit sharp changes of the level density related to the pair breaking. Then the excited states can be approximately labeled by the number of unpaired quasiparticles (seniority). Additional interactions mix the classes of states with different seniority. This mixing along with the finite size effects level off those changes as well as the manifestations of the phase transition occurring as excitation energy increases. This does not contradict to the survival of remnants of pairing correlations in the structure of the eigenfunctions. The presence of correlations in chaotic wave functions due to the two-body nature of the interaction was stressed earlier [13,14]. Another and very important signature of correlations is a regular behavior of strength for specific simple operators as a function of excitation energy, for example in the case of Gamow-Teller transitions [15], or the accumulation of the strength in the form of giant resonances. The latter are essentially analogs of scars known in simple model systems used for studying quantum chaos [16]. Similarly, we expect the tail of pairing correlations to stretch in the chaotic region beyond the formal point of the BCS or HFB phase transition.

One also needs to mention that small systems with their exact constants of motion, such as angular momentum, parity, and isospin in nuclei, have their specific features not reflected in macroscopic approaches. First, these exact conservation laws bring in additional correlations between the classes of states governed by the same Hamiltonian [17,18]. Second, at high level density, complicated schemes of vector coupling serve as a source of geometric chaoticity [19,20] unrelated to the residual interaction. Finally, the nonzero angular momentum is in some sense similar to the magnetic field destroying superconducting pair correlations, although it acts differently from an external field.

The nuclear shell model provides a convenient testing ground for studying both single-particle and collective features

as well as the evolution of complexity and chaos in a function of excitation energy and angular momentum [11,19,21]. The semiempirical effective Hamiltonians fitted by the spectroscopic information available in the lowest part of the spectrum nicely reproduce the multitude of experimental data [22–24]. Using the same Hamiltonians for the many-body problem at higher excitation energy, we expect that the statistical properties of the energy spectrum and the structure of the eigenstates in the model will reflect the actual features of nuclear dynamics. The typical dimensions of such calculations are sufficiently large to reduce statistical fluctuations. At the same time, the results can be rapidly and effectively analyzed.

From the conventional point of view, the pairing correlations are caused by the enhanced attractive two-body matrix elements $\langle (j_2^2)_{J=0}|V|(j_1^2)_{J=0}\rangle$ corresponding to the self-energy of the monopole pair ($j_1 = j_2$) or to the coherent pair transfer between the orbitals j_1 and j_2. In light nuclei, neutrons and protons occupy the same orbitals. Assuming the $j-j$ coupling and exact isospin symmetry, one can expect the dominance of the pairing in the pair state with isospin $T = 1$ [25] (another possibility is the isoscalar spin-triplet pairing of a quasideuteron type with the $L = 0$, $S = 1$, $T = 0$ pairs). The isospin-invariant pairing is important for the symmetric ($N \approx Z$) nuclei near the proton drip line [26,27]. The pairing is also the main interaction making many neutron-rich nuclei particle-stable. It was studied in the group-theoretical models [28] as well as in various microscopic calculations [25,29]. The temperature evolution of the isoscalar and isovector pairing was investigated in the shell model [26] with the realistic Hamiltonian using the Monte Carlo techniques; such approaches, however, are useless for the purpose of studying the properties of individual wave functions.

An important advantage of the shell-model analysis compared to the BCS or HFB approximations is that all constants of motion, particle number, total angular momentum, and isospin, are exactly conserved, and therefore one does not need any additional efforts for restoring correct symmetry of the states. The results can thus be analyzed for a specific class of states in a specific nucleus [11,30]. Solving the shell model explicitly in the truncated Hilbert space we obtain the eigenfunctions which contain all interaction effects including pairing, with the conservation laws strictly fulfilled. Therefore we do not need any additional mean field approximations. With no external heat bath, the phase transition, if it does exist, should manifest itself through the change of the properties of individual eigenstates as a function of excitation energy, or of an equivalent intrinsic temperature scale. Indeed, the pairing phase transition was clearly observed [11,31] in the shell-model calculations for $J^\pi T = 0^+0$ states in *sd*-nuclei. Starting with only the pairing interaction in the exact diagonalization [32] one can develop new approximations for other parts of the interaction based on the exact pairing solution. Measuring the sensitivity of exact wave functions to special perturbations [33] one can probe the transitional regions for various pairing modes. Nontrivial features of such results are the important role of non-pairing parts of the residual interaction, which may smear the regular band-like structure of excited states related to the seniority quantum number, and the long fluctuational tail of enhanced pairing correlations beyond the transition point, a generic feature of mesoscopic systems [34,35].

Below we present the results on the pairing properties of *individual eigenstates* in the shell model. We use even-even nuclei as an object of investigation and study the dependence of the pairing correlator for the given class of states $J^\pi T$ on various parameters; we also compare the classes with different nuclear spins J and isospins T. Within each class the results depend upon the type of interaction and the interaction strength. The results indicate an important role played by geometric effects in mesoscopic systems.

II. PAIRING CORRELATOR

As in our first study of the pairing effects [11], we select as a probe the operator of pairing interaction

$$\mathcal{H}_P = \sum_{t=0,\pm1} P_t^\dagger P_t, \tag{1}$$

where the monopole isovector pair operators with the isospin projection t are defined in terms of the fermion operators $a_{jm\tau}$ and $a^\dagger_{jm\tau}$ coupled to the total angular momentum $L = 0$ (we use this notation in order to distinguish the pair angular momentum L from the many-body angular momentum of nuclear states J) and isospin $T = 1$ according to

$$\begin{aligned} P_t &= \frac{1}{\sqrt{2}} \sum_j [\tilde{a}_j \tilde{a}_j]_{L=0,T=1,T_3=t}, \\ P_t^\dagger &= \frac{1}{\sqrt{2}} \sum_j [a_j^\dagger a_j^\dagger]_{L=0,T=1,T_3=t}. \end{aligned} \tag{2}$$

Here the sums are taken over all single-particle spherical orbitals j in truncated shell-model space. For each $a_\lambda \equiv a_{jm\tau}$, where $m = j_z$ and $\tau = \pm 1/2$ are projections of the single-particle angular momentum and isospin, respectively, the time conjugate operator is defined as $\tilde{a}_\lambda = (-)^{j-m} a_{j-m\tau}$, so that $\tilde{\tilde{a}}_\lambda = -a_\lambda$.

The expectation values of the operators (2) are proportional to the energy gap parameter Δ in BCS-like theories using variational wave functions of fermionic condensate. These expectation values identically vanish in exact stationary states with a fixed particle number. The quadratic combination (1) is positively defined and does not vanish even in a normal Fermi-system. However, its excess as compared to the normal background is related to the effects of superfluidity and essentially measures the quantity proportional to $|\Delta|^2$. The pair operators (2) characterize the strength of the pair transfer to the neighboring nuclei which is the best analog of the macroscopic superconducting current [1,36]. The expectation value $\langle\alpha|\mathcal{H}_P|\alpha\rangle$ of the bilinear operator (1) for the eigenstate $|\alpha\rangle$ of A particles gives the total strength for all transitions from an initial state $|\alpha\rangle$ induced by the monopole pair removal to the states of the nucleus with $A-2$ particles (analog of a sum rule). For low-lying states, this quantity can be measured by pair transfer reactions. At higher excitation energy, where individual states are not resolved, the knowledge of the generic behavior of the pair correlator still might be useful in estimating relevant cross sections as well as the

TABLE I. The low lying $J^\pi T = 0^+0$ energy levels (MeV) of ^{28}Si found in the experiment [37] and predicted by the $1s-0d$ shell model.

Exp. [37]	Shell model
0	0
4.98	5.01
6.69	7.24
8.95	9.87
11.14	10.36
12.30	12.17
12.81	12.87
12.97	13.67
13.23	14.19
14.39	14.64

temperature-dependent characteristics, such as the moment of inertia.

Earlier we calculated [11,31] the expectation values $\langle\alpha|\mathcal{H}_P|\alpha\rangle$ for all individual $J^\pi T = 0^+0$ states in two systems, eight valence particles in ^{24}Mg (dimension $d = 325$ states) and 12 valence particles in ^{28}Si ($d = 839$). The Brown-Wildenthal universal sd (USD) set of two-body interaction matrix elements [22] was used that reproduces well the available spectroscopic data in many *sd*-nuclei. For example, all ten 0^+0 states with excitation energy lower than 15 MeV resolved in the experiment [37] in ^{28}Si agree with the shell-model calculations, both in their number and in the level spacings, see Table I.

Below we refer to the two-body interaction matrix elements for $L = 0, T = 1$ pairs as "pairing matrix elements". In the USD Hamiltonian for *sd*-shell nuclei these matrix elements are negative and vary from -1.1 MeV to -3.2 MeV. Their values can be found in Table II. The calculation of $\langle\mathcal{H}_P\rangle$ is facilitated by the fact that it can be treated as a specific residual interaction with the two-body matrix elements

$$\left\langle \left(j_2^2\right)_{LT} \middle| V_P \middle| \left(j_1^2\right)_{LT} \right\rangle = [(2j_1+1)(2j_2+1)]^{1/2}\delta_{L0}\delta_{T1}. \quad (3)$$

Thus, the operator (1) is universal, and its eigenvalues reflect only the structure of corresponding eigenfunctions.

As a reference point for further discussion we show in Fig. 1 the pair correlator (1) calculated in Ref. [11] for all states $J^\pi T = 0^+0$ in the *sd*-model of ^{24}Mg, panels (a), (c), (e) and ^{28}Si, panels (b), (d), (f). In the lower panels (e) and (f), all 63 matrix elements allowed for two-body interactions in the *sd*-space are taken into account in the diagonalization. The upper panels (a) and (b) show the pronounced seniority related

TABLE II. Two-body reduced matrix elements (in MeV) for $L = 0, T = 1$ pair states within the $1s-0d$ shell-model space.

	$s^2_{1/2}$	$d^2_{3/2}$	$d^2_{5/2}$
$s^2_{1/2}$	-2.125	-1.084	-1.325
$d^2_{3/2}$		-2.185	-3.186
$d^2_{5/2}$			-2.820

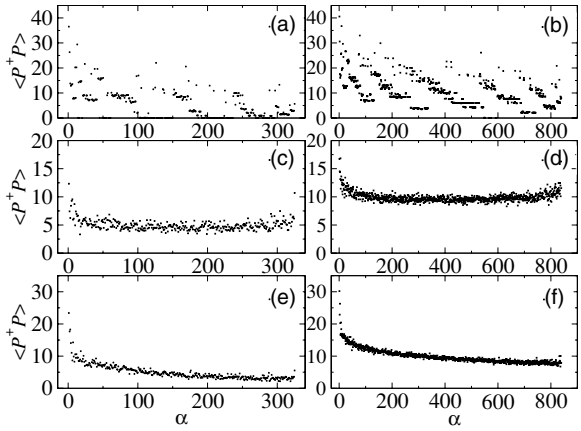

FIG. 1. The pair correlator of Eq. (1) for $J^\pi T = 0^+0$ states in the *sd*-model of ^{24}Mg, panels (a), (c), and (e), and ^{28}Si, panels (b), (d), and (f). The individual points correspond to the eigenstates ordered in increasing energy. Panels (a) and (b) show the results for the pure pairing interaction of Table II, while panels (c) and (d) are calculated for the interaction where the pairing matrix elements are set to zero; the results for the full realistic interaction are given in panels (e) and (f).

structures in the case when the pairing was the only included interaction. The intermediate panels (c) and (d) illustrate the model with pairing interaction excluded from the full set of matrix elements. The eigenstates $|\alpha\rangle$ are ordered in their increasing energy. We summarize the instructive features of these results:

(i) in the full calculation, the pair correlator changes smoothly with excitation energy (or equivalent effective temperature); no appreciable seniority structures are visible;
(ii) the first dozen of low-lying states in lower panels have a significant excess of pair correlations; in the case of ^{28}Si, those are essentially the same states that were found in the previously referred experiment [37];
(iii) the detailed analysis [11] indicates the analog of the smoothed second order phase transition in the end of the sequence of the "paired" states of point (ii);
(iv) beyond the transition point, one still sees a long exponential tail of "fluctuational superconductivity";
(v) the background of the lower plots is close to the results of panels *c* and *d* obtained with no pairing; this corresponds to the normal Fermi-gas behavior with the single-particle occupation numbers found in the shell-model calculation;
(vi) with the pure pairing interaction (and other matrix elements artificially set to zero), Figs. 1(a) and 1(b), the full pattern of seniority families is restored.

We start our new studies with the dependence of the pair correlator on the pairing strength. Figure 2 shows the value of $\langle\mathcal{H}_P\rangle$ for the ground state of ^{24}Mg as a function of an overall scaling factor g introduced into the pairing matrix elements of the residual interaction with $g = 1$ corresponding to the realistic strength of Table II. The nonpairing matrix elements of the full shell model interaction are kept intact.

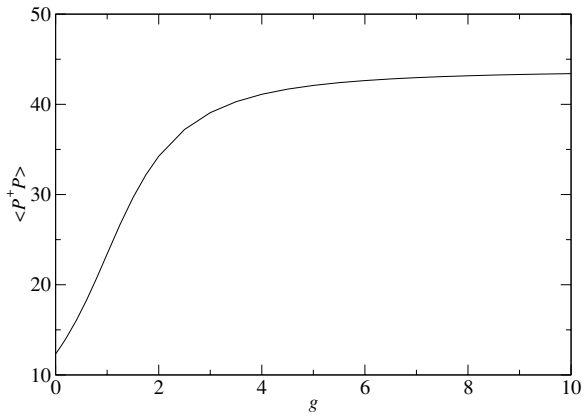

FIG. 2. The pair correlator for the ground state $J^\pi T = 0^+0$ in the *sd*-model of ^{24}Mg as a function of the pairing interaction of Table II scaled with the aid of the overall factor g; other matrix elements are taken from the WB interaction [22].

A typical "smooth phase transition" is seen in Fig. 2 between the two physical limits. In distinction to macroscopic Fermi systems, in finite systems the Cooper condensation does not occur at an arbitrarily weak pairing strength [3]. Below a critical value, $g < g_c$, the BCS theory has only a normal solution with a vanishing order parameter (energy gap). However, in the exact solution, already at no (or weak) pairing, we have a noticeable increase of $\langle \mathcal{H}_P \rangle$ above a pure statistical estimate. Such an estimate can be obtained by taking the average of the operator (1) with the single-particle density matrix characterized by the occupation numbers n_λ. Assuming the time reversal symmetry, $n_{\tilde{\lambda}} = n_\lambda$, that holds for the states with $J = 0$, and identical occupancies for protons and neutrons, we obtain

$$\langle \mathcal{H}_P \rangle = 3 \sum_\lambda n_\lambda^2. \tag{4}$$

The uniform filling, $n = 2/3$, of the lowest $d_{5/2}$ orbital by four protons and four neutrons (the ground state of ^{24}Mg in the extreme independent particle model) would give, according to Eq. (4), $\langle \mathcal{H}_P \rangle = 8$. This number would decrease further if the Fermi surface were smeared and the higher orbitals partially filled.

The equiprobable filling of all orbitals λ takes place at the maximum level density ("infinite temperature" [11,21]) in the centroid of the spectrum. Then $n_\lambda = 1/3$ for ^{24}Mg in the *sd* shell, and this leads to the minimum value of the quantity (4) $\langle \mathcal{H}_P \rangle = 4$, in agreement with the actual values found earlier in the middle of the spectrum, Fig. 1(e). The average value of the operator (1) over the whole Hilbert space (no restriction by angular moment or isospin) can be calculated with simple prescriptions of statistical spectroscopy [38]. For A_v active particles on Ω spin-spatial orbitals,

$$\langle \mathcal{H}_P \rangle = \frac{3}{2(2\Omega - 1)} A_v(A_v - 1), \tag{5}$$

that gives, for $\Omega = 12$ and $A_v = 8$, $\langle \mathcal{H}_P \rangle = 3.7$ in a close agreement with the estimate (4). The observed excess for the ground state at $g = 0$, Fig. 1(c), shows the presence of pairing-like correlations generated by the nonpairing parts of the interaction. Such effects were discussed in detail for quadrupole-quadrupole interaction at a single j-level in Ref. [39]. The increasing chaoticity of excited states [11] rapidly reduces the pairing strength to its statistical value given in Eqs. (4) and (5).

On the other end of the g-dependence, we see the saturation of the pairing strength. At very strong pairing, the single-particle energy spacings are effectively small so that we come to the limit of the isospin-invariant generalization [40,41] of the degenerate seniority model [42] that corresponds to the maximum allowed pairing correlator. Operators P_t and $P_t^\dagger$ of Eq. (2), along with the isospin components, belong to the generators of the $\mathcal{O}(5)$ group which allows one to find the eigenvalues of $\langle \mathcal{H}_P \rangle$. For the lowest $J = 0$ state,

$$\langle \mathcal{H}_P \rangle_T = \tfrac{1}{4} A_v(2\Omega + 6 - A_v) - T(T+1), \tag{6}$$

where T is the total isospin of the many-body state. The maximum possible value of $\langle \mathcal{H}_P \rangle$ for the $1s - 0d$ shell with $\Omega = 12$ and $A_v = 8$ particles corresponds to $\langle \mathcal{H}_P \rangle_0 = 44$. The realistic value $g = 1$ corresponds to the intermediate situation of strong competition between pairing correlations, single-particle excitation energy, mostly due to the spin-orbit splitting, and other residual interactions.

III. PAIRING AS A FUNCTION OF ANGULAR MOMENTUM

Now we discuss the pairing behavior as a function of nuclear spin. The nuclear analog of the Meissner effect (Coriolis antipairing) was predicted [43] shortly after the first applications of the BCS theory to nuclei when it was shown [3,44] that the moment of inertia for low-lying rotational bands in nuclear collective rotation is considerably reduced by pairing compared to the rigid-body value typical for normal Fermi-systems [45]. The semiclassical theory of the nuclear Meissner effect was suggested in [46].

Later it was discovered that, as a rule, the destruction of pairing with increasing spin proceeds in nuclei in a specific way of sequential breaking of the most vulnerable pairs and their alignment along the spin axis [47]. Vast experimental information is accumulated about high spin states where this process is usually seen through band crossings and backbending-type phenomena on the plot of the effective moment of inertia versus rotational frequency. However, the experiment provides only marginal information on the evolution of pairing correlations [48] as a function of nuclear spin. The standard (and practically quite successful) way of interpreting the data uses the cranked deformed shell model [49] with fixed mean field parameters. The rotational bands are built on the intrinsic configurations defined in the body-fixed frame of the deformed nucleus and do not have certain angular momentum. With pairing correlations described in the BCS or HFB approximation, the particle number conservation is also violated. Therefore the analysis in the framework of the shell model approach with strict fulfillment of all conservation laws might be useful.

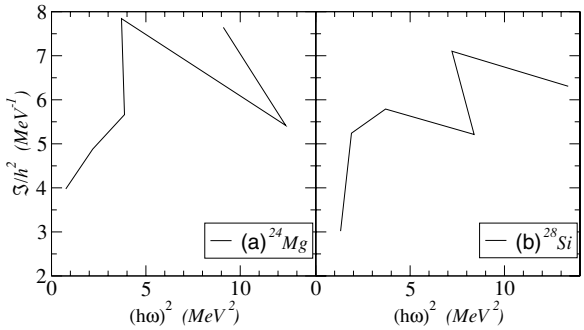

FIG. 3. The ground state band moment of inertia as a function of rotational frequency squared, for ^{24}Mg and ^{28}Si, panels (a) and (b), respectively.

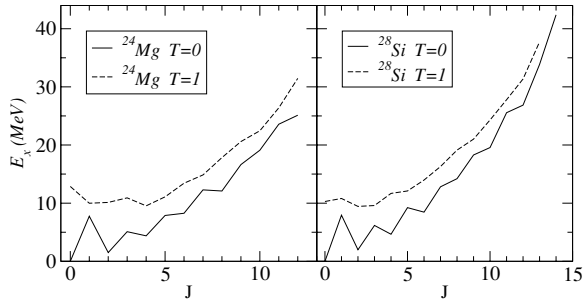

FIG. 4. Comparison of yrast energies for isospin $T = 0$ and $T = 1$ in ^{24}Mg, panel (a), and ^{28}Si, panel (b).

A. Average moment of inertia

The low-lying spectrum of ^{24}Mg is known experimentally. It was repeatedly discussed in the framework of the shell model, cranking model and other approaches, see, for example, [50], and references therein. The *sd*-shell model with the semiempirical interaction [22] predicts the level positions in good agreement with data. We show in Fig. 3(a) the standard plot of the moment of inertia vs rotational frequency squared for the yrast even spin $T = 0$ states. Both, empirical and shell-model, graphs display the strong back-bending at 8^+; there is no reliable experimental candidate for the 10^+ state. This back-bending is well known [50] to reflect the yrast position, 8^+_1, of the aligned configuration. The second 8^+ state, 8^+_2, has the highest calculated transition probability to the 6^+ state, $B(E2; 8^+_2 \to 6^+) = 84.1\ e^2\ \mathrm{fm}^4$, and can be considered as a continuation of the ground state band while for the 8^+_1 state $B(E2; 8^+_1 \to 6^+) = 19.9\ e^2$ fm. However, the situation is not pure because next excited 8^+ states also reveal enhanced $E2$ transitions to the yrast 6^+ state, 33.6 e^2 fm^4 and 3.9 e^2 fm^4, respectively. Effects of nonaxiality and residual interactions increasingly mix the configurations as level density increases and make it impossible to strictly segregate the rotational band. Another nucleus under study in the *sd* shell model is ^{28}Si; it was a testing ground for the ideas of quantum chaos in Ref. [11]. The standard backbending plot for ^{28}Si is shown in Fig. 3(b). Here also there is a good agreement between data and shell model calculations.

With the use of the full solution in the realistic shell model we can investigate the influence of the angular momentum on the pairing properties for all $J^\pi T$ classes of eigenstates with precisely defined constants of motion. First, we consider the yrast states. Figure 4(a) shows the yrast energies for isospin $T = 0$ and $T = 1$ in ^{24}Mg. The $T = 0$ sequence reveals significant odd $J-$ even J staggering; especially the yrast $J = 1^+$ level has too high energy. However, the average behavior of the sequence can be well described with a parabola with the moment of inertia $I \approx 3.1\ \mathrm{MeV}^{-1}$. We can notice that the number is quite close to the rigid body spherical moment of inertia $I_r^\circ = (2/5)AmR^2 \approx 2.8\ \mathrm{MeV}^{-1}$. It is also close to the result for the upper part of the $T = 1$ sequence. A very similar picture can be seen for the shell model calculations in ^{28}Si, Fig. 4(b), where the shell model shows the moment of inertia equal to 2.9 MeV^{-1} and 3.4 MeV^{-1} for $T = 0$ and $T = 1$, respectively, while the rigid body spherical moment of inertia would be 3.6 MeV^{-1}.

Heavier nuclei demonstrate the same trend as was shown in Ref. [51] for tin isotopes where the G-matrix effective interaction [52] was used for shell model calculations. The average moment of inertia along the yrast line, extended to the highest spins, approaches the rigid body value. The mechanism of this reduction of pairing correlations by increasing spin is associated with multiple breaking of Cooper pairs and alignment of particles. As explained by Feynman in application to rotating superfluid helium, the quanta of circulation penetrate the superfluid liquid one by one and the equilibrium rotation of the vortex lattice corresponds to that of a rigid body as the most energetically favorable. In a small Fermi system, as the nucleus, a similar process goes through the increase of average seniority. The result becomes insensitive to the details of the residual interaction since the nucleus is getting close to the normal Fermi-liquid phase that is known to rotate as a rigid body [45].

B. Pair correlator as a function of spin

The full shell model solution allows one to trace the evolution of the pair correlator along any sequence of states in Hilbert space.

1. Yrast states

Figure 5 illustrates the change of the pair correlator for the yrast states in ^{28}Si, in two classes of states, $T = 0$, Fig. 5(a), and $T = 1$, Fig. 5(b). Again, the even-J–odd-J staggering indicates the difference in structure of corresponding yrast states. However, the average behavior of the pair correlator is quite similar in both isospin classes. The results for ^{24}Mg, Figs. 5(c) and 5(d), show the same generic pattern.

In all cases considered, the parametrization of the pair correlator as a function of yrast spin can be taken as

$$\langle \mathcal{H}_P(J) \rangle = \langle \mathcal{H}_P(0) \rangle \left[1 - \frac{J(J+1)}{B} \right]^2. \qquad (7)$$

The numerical values of the parameters in Eq. (7) are given in Table III.

Such a dependence on angular momentum was long ago predicted in a semiclassical consideration of rotating

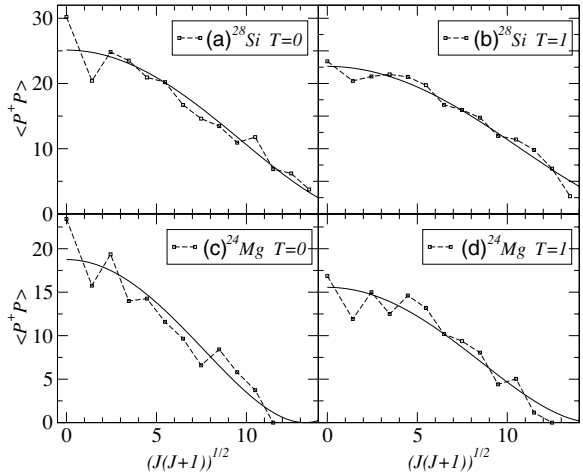

FIG. 5. The pair correlator for the yrast shell model states, in ^{28}Si, panels (a) ($T = 0$) and (b) ($T = 1$), and ^{24}Mg, panels (c) ($T = 0$) and (d) ($T = 1$).

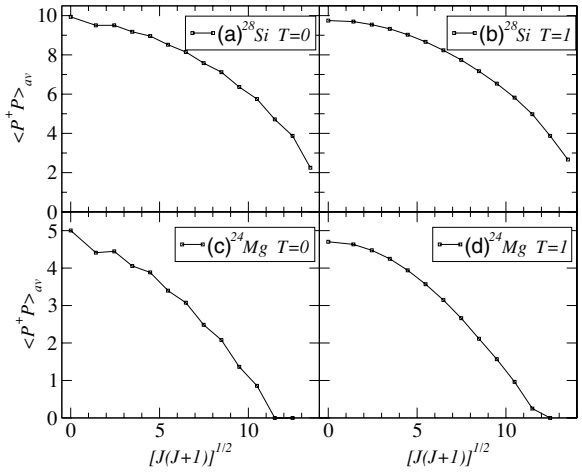

FIG. 6. The pair correlator in the *sd* shell model of ^{28}Si and ^{24}Mg averaged over all states of given spin J for $T = 0$, panels (a) and (c), and $T = 1$, panels (b) and (d).

superfluid nuclei by Grin' and Larkin [46]. In this theory, the pairing gap $\Delta(J)$ changes with spin J (in the spirit of the model, this evolution has to be taken along the yrast line of the nucleus) as

$$\Delta(J) \approx \Delta(0)\left[1 - \frac{J(J+1)}{J_c^2}\right]. \tag{8}$$

Assuming that our pair correlator (1) is proportional to Δ^2, we come to the expression (8). The critical spin J_c in semiclassical theory [46] can be estimated as

$$J_c = a\,\frac{\Delta(0) I_r}{l_0}, \tag{9}$$

where a is a numerical factor, $a \approx 2/2.5$, I_r the rigid body moment of inertia and l_0 the single-particle orbital momentum at the Fermi surface. Equation (9) has a clear meaning: at this condition the Coriolis force creates a perturbation of the order of the pairing gap. The shell model results qualitatively agree with the estimate Eq. (9). Assuming that the moment of inertia is the quantity that is changing most from ^{24}Mg to ^{28}Si, we predict the ratio $J_c(\mathrm{Si})/J_c(\mathrm{Mg}) = 1.27$ that is coincides with what comes from the corresponding values of the parameter B in Table III.

However, Eq. (9), taken literally, would predict for ^{24}Mg with $I_r = 2.8\,\mathrm{MeV}^{-1}$, $a \approx 2.5$, $l_0 \approx 2$, and $\Delta(0) \approx 2\,\mathrm{MeV}$ (the BCS calculation gives the average over the orbitals value of Δ equal to 2.3 MeV for ^{24}Mg and 1.9 MeV for ^{28}Si) the critical spin $J_c \approx 8$ that is significantly lower than the value 13 given by Table III. The semiclassical theory, as any mean field approach, predicts a phase transition in $\Delta(J)$ similar to that for the critical magnetic field in bulk superconductors. However in a small system the fluctuational effects exclude a sharp disappearance and slope singularity of the order parameter. Instead, we again see the tail in the region of J close to J_c, where the semiclassical theory does not work. The parameter B in Eq. (7) is determined by the geometry of the shell model space rather than by the Coriolis forces.

TABLE III. Parameters of Eq. (2), the change of the pair correlator along the yrast line for ^{24}Mg and ^{28}Si.

A	T	$\langle \mathcal{H}_P(0) \rangle$	B
24	0	18.75	175.9
24	1	15.56	220.7
28	0	25.12	285.7
28	1	22.62	344.8

2. *Average pair correlator*

The full shell model solution provides another interesting information if one looks at the pair correlator averaged over *all states* in a given JT class. Figures 6(a) and 6(b) show the result of such averaging as a function of J for the states with $T = 0$ and $T = 1$, respectively, in ^{24}Mg. There is no considerable difference in the behavior of the pair correlator for these two isospin values. The absolute value of $\langle \mathcal{H}_P \rangle$ is only 20% of what we had had for the yrast states. At $J = 0$, this value is 4.74 for $T = 0$ and 4.81 for $T = 1$ states. This means that here we deal with the normal Fermi-gas pair fluctuations rather than with the superfluid pair condensate. Nevertheless, the J-dependence still can be well described in the same way as in Eq. (7). The critical parameter is the same for the two isospin classes, $B = 200.3$ for $T = 0$ and $B = 200.8$ for $T = 1$, taking an average value between the values of this parameter for $T = 0$ and $T = 1$ along the yrast-line, Table III.

The maximum possible spin of the *sd* configuration is $J_{max} = 12$ for ^{24}Mg and 14 for ^{28}Si. If one defines $B = J_c(J_c + 1)$, we can formally find here $J_c \approx 14 > J_{max}$ for ^{24}Mg. This means that there is no sharp cutoff in the behavior of the pair correlator, and the semiclassical theory cannot describe the tail emerging because of the finite size of the system.

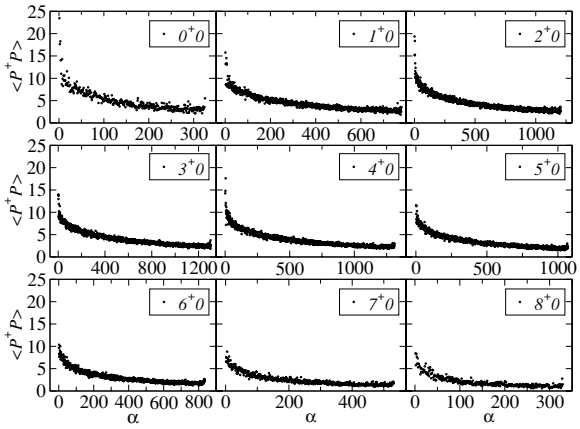

FIG. 7. The pair correlator in the *sd* shell model of ^{24}Mg averaged over all states of spins from $J = 0$ to $J = 8$ and $T = 0$.

3. Global behavior

Now we look at the global behavior of the pair correlator through the properties of individual wave functions found in the shell model. The pair correlator was calculated for all states $|J^+,\ T = 0\rangle$ of positive parity in the *sd* shell model for ^{24}Mg and ^{28}Si. The $J^\pi = 0^+$ states, as well as the yrast states and the average values of the pair correlator, were discussed earlier. Here we show, Fig. 7, the whole picture for all states in ^{24}Mg with different values of nuclear spin, from $J = 8$ to $J = 9$, where the dimension is sufficiently large to reveal statistical trends. For all values of spin, the pair correlator is plotted as a function of the state number with the states ordered in increasing excitation energy.

The main conclusion that follows from Fig. 7 is that the pair correlator as a function of excitation energy behaves qualitatively similarly for all J-classes. In the classes with larger dimensions, the fluctuations are noticeably suppressed, and the pair correlator can be considered as a function of excitation energy, i.e., a *thermodynamic variable*. In the statistical analysis of the shell model wave functions [11], we have found that the degree of complexity of the eigenstates can be conveniently measured by their information entropy in the mean field (original shell-model) basis. The smooth behavior of information entropy can also be interpreted as the indication that the complexity of the eigenstates shows thermodynamic features. This was understood as a result of *chaotic mixing* of the basis states that leads to the equilibration of macroscopic properties of the eigenstates in a given energy window [19,53]. The same was valid for the occupancies of the single-particle orbitals (see also similar results for complex atoms [54]). Looking at the pair correlator, we encounter the manifestation of the mixing for a pure dynamical quantity. The thermodynamics of finite nuclei is a subject of ongoing discussions, see, for example, [55,56]. The full many-body solution shows that equilibration of macroscopic observables results from the residual interaction in the absence of any external heat bath. In other words, this interaction plays the role of a heat bath for measurements with the aid of a single-particle thermometer [19,21,57].

All classes of states with different spins reveal an enhanced pair correlator for few low-lying states and the exponential tail of diminishing correlations at high level density. Since the variations of the correlator between the adjacent spin classes are relatively small, we can attempt to make estimates using the smooth statistical description of semiclassical nature that was suggested earlier [20] for a system governed by *random interactions*. The quantum vector coupling of individual particle spins into total angular momentum presents a hard problem but can be approximately circumvented by the statistical approach based on the ideas of geometric chaoticity [11,18,20,60]. In the high level density region, the occupation numbers of single-particle orbitals, in spite of the strong interaction between the particles and, in some sense, due to this interaction, can be described by the Fermi-Dirac statistics as was shown for complex atoms [54] and nuclei [11,19]. We consider the aligned states of spin J and its projection $M = J$. In order to take into account the difference between the spin classes, we introduce a Lagrange multiplier γ related to the angular momentum conservation and assume that the occupation numbers (the same for protons and neutrons in our cases) can be written as

$$n_{jm} = \frac{1}{\exp[\beta\epsilon_j + x + \gamma m] + 1}, \tag{10}$$

where ϵ_j are effective single-particle energies, β is inverse thermodynamic temperature related to excitation energy, whereas the chemical potential $\mu = -x/\beta$ and the effective cranking frequency γ/β are to be found from the conservation of the particle number A and the total angular momentum projection M,

$$A = 2\sum_{jm} n_{jm}, \quad M = 2\sum_{jm} m n_{jm}. \tag{11}$$

As shown in Ref. [20], the dependence of occupation numbers on M is mild (close to linear), except for the region near the full alignment, $J = J_{\max}$. In the semiclassical region, $1 \ll J \ll J_{\max}$, we can use the expansion in the parameter γ (due to time-reversal invariance of the starting $J = 0$ state, the chemical potential has a correction x_2 of the second order in γ) and obtain

$$n_{jm} \approx n_j^\circ\big[1 - \big(1 - n_j^\circ\big)\gamma m + \tfrac{1}{2}\big(1 - n_j^\circ\big)\big(1 - 2n_j^\circ\big)\gamma^2 m^2 + \big(1 - n_j^\circ\big)x_2\big], \tag{12}$$

where n_j° are the M-independent occupancies for $J = 0$.

The results are readily expressed in terms of the sums depending on the original self-consistent occupancies n_j°,

$$f_1 = \sum_{jm} n_j^\circ\big(1 - n_j^\circ\big), \quad f_2 = \sum_{jm} \big(n_j^\circ\big)^2\big(1 - n_j^\circ\big), \tag{13}$$

$$g_1 = 2\sum_{jm} n_j^\circ\big(1 - n_j^\circ\big)m^2, \tag{14}$$

$$g_2 = \sum_{jm} n_j^\circ\big(1 - n_j^\circ\big)\big(1 - 2n_j^\circ\big)m^2, \tag{15}$$

$$g_3 = \sum_{jm} \big(n_j^\circ\big)^3\big(1 - n_j^\circ\big)m^2, \tag{16}$$

where $\sum_m m^2 = j(j+1)(2j+1)/3$. The combination $n_j^\circ(1-n_j^\circ)$ in these equations is a usual fluctuation of the particle occupation numbers near the Fermi surface; being multiplied by $j(j+1)$ it provides the corresponding fluctuation of angular momentum. The self-consistency conditions (11) determine the variational parameters

$$\gamma = -\frac{M}{g_1}, \quad x_2 = \frac{\gamma^2 g_2}{2f_1}. \tag{17}$$

The pair correlator in this statistical approximation is given by the generalization of the previously used expression Eq. (4),

$$\langle \mathcal{H}_P \rangle = 3 \sum_{jm} n_{jm} n_{j-m}, \tag{18}$$

so that at $J = 0$

$$\langle \mathcal{H}_P \rangle_0 = 3 \sum_j \left(n_j^\circ\right)^2 (2j+1). \tag{19}$$

As J increases, the numerical value of the correlator goes down because the construction of the aligned state requires the violation of the time-reversal symmetric occupation, preferential filling of orbitals with positive projections M and devastating their time-conjugate partners. With the aid of the expansion (12) we come to

$$\langle \mathcal{H}_P \rangle_M = 3 \sum_{jm} \left(n_j^\circ\right)^2 \left[1 - n_j^\circ\left(1-n_j^\circ\right) \times \gamma^2 m^2 + 2\left(1-n_j^\circ\right)x_2\right]. \tag{20}$$

Identifying the projection of the aligned state with its spin, $M^2 \to \mathbf{J}^2$, and using the self-consistency conditions (17), we predict the spin dependence of the pair correlator in the semiclassical region,

$$\langle \mathcal{H}_P \rangle_J = \langle \mathcal{H}_P \rangle_0 [1 - CJ(J+1)], \tag{21}$$

where

$$C = \frac{3[g_3 + g_2(f_2/f_1)]}{g_1^2 \langle \mathcal{H}_P \rangle_0}. \tag{22}$$

This purely statistical estimate predicts a behavior of the pair correlator close to what is seen in the exact calculations in the middle of the spectra. In the finite shell model space the central part corresponds to "infinite temperature" so that the right half of the shell model spectra can be described by negative temperatures (preferential occupation of higher orbitals). In the middle the single-particle orbitals are filled evenly so that n_j° are equal to 1/3 in ^{24}Mg and 1/2 in ^{28}Si. This gives the value of $\langle \mathcal{H}_P \rangle_0 = 4$ in ^{24}Mg and 9 in ^{28}Si, while the shell-model values are 4.13 and 9.43. For this degree of filling, the constant C, Eq. (22), is equal to 0.0082 and 0.0036 for ^{24}Mg and ^{28}Si, respectively. Estimating the value of C from computed data Eq. (21) in the semiclassical region of $J \geqslant 5$ we get corresponding values 0.0084 ± 0.0005 and 0.0041 ± 0.0001. This close agreement shows that the approach starting with the statistical mean field reasonably well describes the central part of the spectrum.

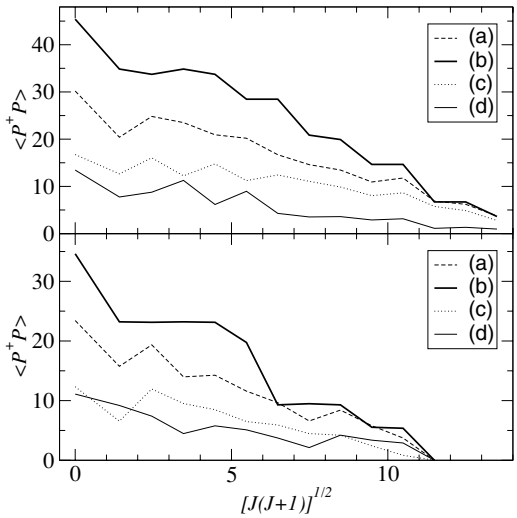

FIG. 8. Pair correlator for $T = 0$ yrast states in the *sd* shell model for ^{24}Mg (lower panel) and ^{28}Si (upper panel) as a function of nuclear spin: full interaction, dashed line (a); pure pairing interaction case, thick solid line (b); only nonpairing parts of the interactions, dotted line (c); and the difference (a)–(c) of the full interaction and the nonpairing part, thin solid line (d).

IV. PAIRING AND OTHER INTERACTIONS

The interplay of pairing with other components of residual interactions is by no means trivial. In the standard BCS theory the influence of the nonpairing parts of interactions is essentially ignored, except for the given parameters of the mean field. In the HFB approach, the mean field is found self-consistently in both channels, particle-particle and particle-hole. The interplay of interactions in the excited states can be added within the random phase approximation (RPA). The full shell model results do not always agree with these simple notions. Below we illustrate the situation with typical examples.

A. Pairing from nonpairing interactions

We have already seen in our reference plot, Fig. 1, that the global picture of the pairing correlator in a function of excitation energy is strikingly different for a pure pairing case and for the full shell model calculation. The first impression is that non-pairing parts of the interaction just destroy the coherent pattern of seniority families characteristic for the pure pairing. Let us, however, look at Fig. 8.

In the earlier discussed case of the pure pairing interaction, line (b), the correlator reaches its largest value, except for the maximum spin. In the full shell model calculation with the entire residual interaction, line (a), the correlator behaves in a similar way as a function of spin along the yrast line but at a lower level. However, even without pairing forces at all, line (c), considerable pairing correlations are still present, repeating the same staggering pattern. Roughly speaking, in the full interaction case, the net contribution of pairing is reduced to the difference of (a) and (c), see line (d). Of course, such a mechanical subtraction is not valid and the

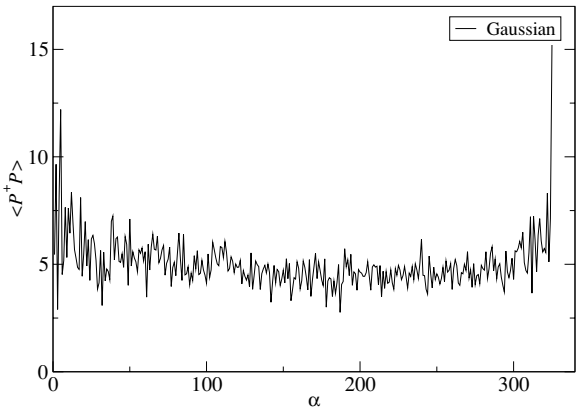

FIG. 9. Pair correlator for $J = 0, T = 0$ states in the *sd*-shell model of ^{24}Mg calculated with the realistic single-particle energies and random matrix elements of residual interaction taken from the Gaussian distribution with zero mean.

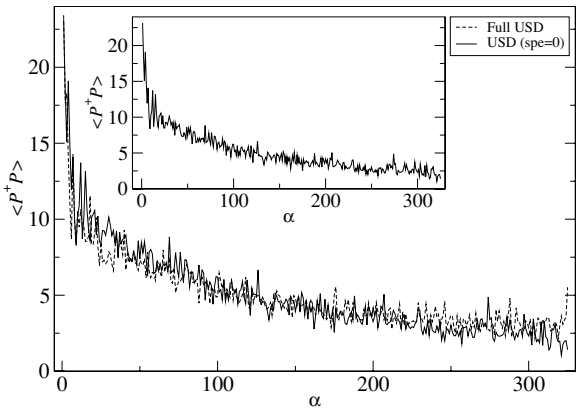

FIG. 10. Pair correlator for $J = 0, T = 0$ states in the *sd* shell model of ^{24}Mg calculated with the degenerate single-particle energies and realistic matrix elements of residual interaction (solid line) compared with the results of the full USD interaction (dashed line).

interplay of different components of the interaction is much more complicated.

As discussed in detail in [51], the kinematic relations between the particle-particle and particle-hole channels in a system of interacting fermions do not allow one to simply separate the contributions of various components. Even a pure quadrupole-quadrupole interaction, being translated into the particle-particle channel, contains a significant component of monopole pairing. The old models "pairing plus quadrupole interaction" could work only on the level of the mean field, and more precisely, Hartree approximation. Being used for full calculation, such models contain nonphysical components contradicting to Fermi statistics and need to be properly antisymmetrized. In fact, the role of non-pairing parts of the interaction is twofold: the incoherent processes destroying the pairs coexist with the rearrangement and higher order effects reviving the pairing.

B. Pairing from random interactions

The apparent signatures of order in the shell-model systems governed by random interactions were found in Ref. [58] and immediately triggered an avalanche of articles, see review papers [18,59,60]. As suggested in [20,61], the predominance of the ground state spin $J_0 = 0$, as well as the enhancement of the probability of maximum possible ground state spin, $J_0 = J_{max}$, is mainly related to the geometry of system that is respected by any random but rotationally invariant two-body interaction. The effective Hamiltonian averaged over random parameters depends on the characteristics of the classes of the states, such as spin and isospin. This fact leads to the exaggerated weight of the edge values of angular momentum.

The subsequent work showed that there are effects in excess of the geometric chaoticity. Although the ground states with $J_0 = 0$ in a system with random interactions have only a small overlap with the fully paired states [20,61] and a distribution function of the ground state components in the shell model basis reminds what is expected for a wave function taken as a random vector in Hilbert space, there is still an enhancement noticed in a realistic shell model with random parameters [61]. These dynamical effects show that essentially any rotationally invariant interaction generates in high order processes some pairing correlations. Figure 9 shows the pair correlator for $J^\pi T = 0^+0$ states in ^{24}Mg in the case when all 63 independent two-body matrix elements of rotation- and isospin-invariant residual interaction were taken randomly from the Gaussian distribution with zero mean and the same variance. For the majority of states the pair correlator is on the level typical for the fluctuations in the Fermi gas, see above. A significant increase for the lowest and the highest states shows the increased role of pairing (original and induced) in the states with a lower degree of complexity. The randomness of the sign of interaction leads to the symmetry between the lowest and the highest states.

It was shown [11] that the mean field with its spectrum of single-particle energies stabilizes the regular components of the eigenstates. In the degenerate case, when all single-particle levels are set to the same value, any residual interaction is getting effectively strong, and information entropy reaches, for the majority of the eigenstates, the chaotic level typical for the Gaussian orthogonal ensemble. In this case the spectral evolution can be seen [11,21] only at the edges of the spectrum. Figure 10 presents the pair correlator for 0^+0 states in ^{24}Mg calculated for the degenerate limit. The picture is similar to the one found with the random interactions, Fig. 9. This means that, in the absence of the skeleton built by the mean field, the rapidly increasing level density makes the system chaotic for any physically reasonable interaction. The pairing effects, in excess to the normal Fermi-gas fluctuations, survive only in the regions of lower level density. This emphasizes the role of incoherent interactions and at the same time underlines the contrast of our mesoscopic case against the bulk superconductivity.

V. CONCLUSION

We considered, numerically and with the aid of simple analytical models, the pairing phase transition in the framework of

a nuclear shell model. This model provides a typical situation for a mesoscopic system with a mean field and reasonably strong residual interaction. The phase transition is measured by the behavior of the pair correlator (in our example for isospin invariant pairing with quantum numbers $J = 0,\ T = 1$) for all individual quantum states in the shell-model space. The pair correlator is studied as a function of pairing strength, excitation energy and spin both for realistic interaction Hamiltonian and for an ensemble of random interactions.

The main conclusions can be summarized as follows.

(i) The pair correlator for individual states exhibits a regular behavior as a function of excitation energy with a clear transition from an enhanced value around the ground state to a background value for highly excited states. Because of strong mixing of simple configurations, we can not only expect the level repulsion and spectral rigidity as generic signatures of quantum chaos, but also the equilibration of dynamic properties of neighboring states. They indeed "look the same" [53].

(ii) The transition is smooth as expected for a finite mesoscopic system and reveals a long exponential tail of pair correlations beyond what could be called the phase transition region.

(iii) The pattern is very similar in all classes of states of different total spin with the gradual reduction of the total curve for higher spins.

(iv) The values of the correlator in the chaotic region near the middle of the spectrum can be approximately predicted by the simple semiclassical model with average occupation numbers of single-particle orbitals.

(v) Pairing in a finite system is considerably influenced by the nonpairing parts of the interparticle interaction.

(vi) Our numerical results are obtained in a certain version of the shell model based on a specific truncation of single-particle space and a selected residual interaction. Therefore they are model dependent. However, the model respects all conservation laws, it is solved exactly and well tested for realistic nuclei in the low-energy region. As excitation energy and level density increase, the model reveals typical features of many-body quantum chaos in agreement with random matrix theory. This allows us to expect that the qualitative results of the model reflect generic properties of pairing phase transitions in mesoscopic environment.

(vii) A question of application to loosely bound nuclei requires an additional consideration. The admixtures of weakly bound states with large spatial structure as well as virtual states in the continuum can significantly change the pairing properties.

ACKNOWLEDGMENTS

The authors acknowledge support from the NSF grant PHY-0555366. Some of the calculations were possible due to the NSF MRI grant PHY-0619407. We thank B. A. Brown and A. Volya for numerous discussions.

[1] A. Bohr and B. Mottelson, *Nuclear Structure*, Vol. 1 (Benjamin, New York, 1969).
[2] A. Bohr, B. Mottelson, and D. Pines, Phys. Rev. **110**, 936 (1958).
[3] S. T. Belyaev, Mat. Fys. Medd. Dan. Vid. Selsk. **31**, No. 11 (1959).
[4] D. J. Dean and M. Hjorth-Jensen, Rev. Mod. Phys. **75**, 607 (2003).
[5] T. Tsuboi and T. Suzuki, J. Phys. Soc. Japan **43**, 444 (1977).
[6] C. R. Leavens and E. W. Fenton, Phys. Rev. B **24**, 5086 (1981).
[7] J. A. Sheikh, R. Palit, and S. Frauendorf, Phys. Rev. C **72**, 041301(R) (2005).
[8] Y. R. Shimizu, J. D. Garrett, R. A. Broglia, M. Gallardo, and E. Vigezzi, Rev. Mod. Phys. **61**, 131 (1989).
[9] B. Lauritzen, A. Anselmino, P. F. Bortignon, and R. A. Broglia, Ann. Phys. (NY) **223**, 216 (1993).
[10] V. Zelevinsky, M. Horoi, and B. A. Brown, Phys. Lett. **B350**, 141 (1995).
[11] V. Zelevinsky, B. A. Brown, N. Frazier, and M. Horoi, Phys. Rep. **276**, 85 (1996).
[12] T. Døssing *et al*., Phys. Rev. Lett. **75**, 1276 (1995).
[13] T. A. Brody *et al*., Rev. Mod. Phys. **53**, 385 (1981).
[14] V. V. Flambaum, G. F. Gribakin, and F. M. Izrailev, Phys. Rev. E **53**, 5729 (1996).
[15] N. Frazier, B. A. Brown, D. J. Millener, and V. Zelevinsky, Phys. Lett. **B414**, 7 (1997).
[16] L. Kaplan and E. J. Heller, Phys. Rev. E **59**, 6609 (1999).
[17] M. Horoi, A. Volya, and V. Zelevinsky, Phys. Rev. C **66**, 024319 (2002).
[18] V. Zelevinsky and A. Volya, Phys. Rep. **391**, 311 (2004).
[19] V. Zelevinsky, Annu. Rev. Nucl. Part. Sci. **46**, 237 (1996).
[20] D. Mulhall, A. Volya, and V. Zelevinsky, Phys. Rev. Lett. **85**, 4016 (2000).
[21] M. Horoi, V. Zelevinsky, and B. A. Brown, Phys. Rev. Lett. **74**, 5194 (1995).
[22] B. A. Brown and B. H. Wildenthal, Annu. Rev. Nucl. Part. Sci. **38**, 29 (1988).
[23] B. A. Brown, Prog. Part. Nucl. Phys. **47**, 517 (2001).
[24] E. Caurier, G. Martinez-Pinedo, F. Nowacki, A. Poves, and A. P. Zuker, Rev. Mod. Phys. **77**, 427 (2005).
[25] A. L. Goodman, Adv. Nucl. Phys. **11**, 263 (1979).
[26] D. J. Dean, S. E. Koonin, K. Langanke, P. B. Radha, and Y. Alhassid, Phys. Rev. Lett. **74**, 2909 (1995); D. J. Dean, Proceedings of the Conference on Nuclear Structure at the Limits, ANL/PHY-97/1, p. 232.
[27] G. Martinez-Pinedo, K. Langanke, and P. Vogel, Nucl. Phys. **A651**, 379 (1999).
[28] J. A. Evans, G. G. Dussel, E. E. Maqueda, and R. P. J. Perazzo, Nucl. Phys. **A367**, 77 (1981); G. G. Dussel, E. E. Maqueda, R. P. J. Perazzo, and J. A. Evans, *ibid.* **A450**, 164 (1986).
[29] W. Satula and R. Wyss, Phys. Rev. Lett. **86**, 4488 (2001); **87**, 052504 (2001).
[30] B. A. Brown *et al*., OXBASH code, MSUNSCL Report 524 (1988).
[31] V. G. Zelevinsky, Proceeding of the Conference on Nuclear Structure at the Limits, ANL/PHY-97/1, p. 353.
[32] A. Volya, B. A. Brown, and V. Zelevinsky, Phys. Lett. **B509**, 37 (2001).
[33] A. Volya and V. Zelevinsky, Phys. Lett. **B574**, 27 (2003).

[34] A. Mastellone, G. Falci, and R. Fazio, Phys. Rev. Lett. **80**, 4542 (1998).
[35] A. Larkin and A. Varlamov, *Theory of Fluctuations in Superconductors* (Oxford University Press, Oxford, 2004).
[36] D. R. Bes, R. A. Broglia, O. Hansen, and O. Nathan, Phys. Rep. **34C**, 1 (1977).
[37] J. Brenneisen *et al*., Z. Phys. A **351**, 430 (1995); **351**, 443 (1995); **351**, 352 (1995).
[38] J. B. French and K. F. Ratcliff, Phys. Rev. C **3**, 94 (1971); K. F. Ratcliff, *ibid*. **3**, 117 (1971).
[39] A. Volya, Phys. Rev. C **65**, 044311 (2002).
[40] K. T. Hecht, Phys. Rev. **139**, B794 (1965).
[41] J. P. Elliott and J. A. Evans, Phys. Lett. **B31**, 157 (1970).
[42] G. Racah, Phys. Rev. **76**, 1352 (1949).
[43] B. R. Mottelson and J. G. Valatin, Phys. Rev. Lett. **5**, 511 (1960).
[44] A. B. Migdal, Nucl. Phys. **13**, 655 (1959).
[45] R. M. Rockmore, Phys. Rev. **118**, 1645 (1960).
[46] Yu.T. Grin' and A. I. Larkin, Yad. Fiz. **2**, 40 (1965) [Sov. J. Nucl. Phys. **2**, 27 (1965)].
[47] F. S. Stephens and R. S. Simon, Nucl. Phys. **A183**, 257 (1972).
[48] J. D. Garrett *et al*., Phys. Rev. Lett. **47**, 75 (1981).
[49] R. Bengtsson and S. Frauendorf, Nucl. Phys. **A314**, 27 (1979); **A327**, 139 (1979).
[50] R. K. Sheline, I. Ragnarsson, S. Åberg, and A. Watt, J. Phys. G **14**, 1201 (1988).
[51] A. Volya, V. Zelevinsky, and B. A. Brown, Phys. Rev. C **65**, 054312 (2002).
[52] A. Holt, T. Engeland, M. Hjorth-Jensen, and E. Osnes, Nucl. Phys. **A634**, 41 (1998).
[53] I. C. Percival, J. Phys. B **6**, L229 (1973).
[54] V. V. Flambaum, A. A. Gribakina, G. F. Gribakin, and M. G. Kozlov, Phys. Rev. A **50**, 267 (1994).
[55] Ph. Chomaz and F. Gulminelli, in *Nuclei and Mesoscopic Physics, WNMP 2004*, edited by V. Zelevinsky, AIP Conf. Proc. No. 777 (AIP, New York, 2005), p. 209.
[56] A. Schiller *et al*., in [55], p. 216.
[57] V. V. Flambaum and F. M. Izrailev, Phys. Rev. E **56**, 5144 (1997).
[58] C. W. Johnson, G. F. Bertsch, and D. J. Dean, Phys. Rev. Lett. **80**, 2749 (1998).
[59] Y. M. Zhao, A. Arima, and N. Yoshinaga, Phys. Rep. **400**, 1 (2004).
[60] T. Papenbrock and H. A. Weidenmüller, nucl-th/0701092.
[61] M. Horoi, B. A. Brown, and V. Zelevinsky, Phys. Rev. Lett. **87**, 062501 (2001).